Experimental study of coherence and correlation in the anisotropy of Ne *KL-LLL* satellite Auger decay

László Tóth,* Sándor Ricz, Endre Takács,† Béla Sulik, János Végh, and Imre Kádár
Institute of Nuclear Research of the Hungarian Academy of Sciences (ATOMKI), P.O. Box 51, H-4001 Debrecen, Hungary‡
(Received 9 January 2004; published 11 June 2004)

The coherent excitation of overlapping atomic states by ion projectiles has a strong effect on the angular distribution of Auger electrons. Therefore, the measurement of the angular anisotropy of outgoing Auger electrons is suitable for the quantitative studies of the influence of the coherence. In our experiment the Ne target was bombarded with 700–2000 keV H^+ and 2000 keV He^+ projectiles. The angular distributions of $KL_{2,3}$-$LLL_{2,3}$ Auger electrons emitted from the decay of the coherently excited $1s2p$ doubly vacancy states of Ne were measured. The anisotropy parameter of the Auger decay was deduced from the measurements and compared with theoretical results calculated using the multiconfiguration Dirac-Fock method. The results indicate that one should go beyond the *LS* coupling scheme even at this relatively low atomic number element, but also suggest that only partially overlapping states need to be taken into account.

DOI: 10.1103/PhysRevA.69.062708 PACS number(s): 34.90.+q

I. INTRODUCTION

Inner-shell ionization and excitation studies by photon and particle beams provided results about the Auger decay process in recent years. The energy, intensity, and angular anisotropy of the Auger-electron emission provides information both about the excitation process and the dynamics of the decay. Angular distribution and spin-polarization studies are sensitive to the finest details, even about coherently excited overlapping states [1].

The angular anisotropy of the Auger-electron emission depends on many-electron effects, the coupling of spin and orbital angular momenta in the initial and final states, and dynamical effects like relaxation and final state channel interaction. It has long been pointed out [1] that coherent excitation of atomic states can lead to quantum-interference effects that strongly influence the structure and relaxation properties of these systems. Coherence between nondegenerate states are generally neglected in simple theories, although they can lead to effects like quantum beats in the time dependence of the photonic decay [2] or can modify the anisotropic angular distribution of the decay products [3]. In order to coherently excite nondegenerate levels some kind of a mixing should exist between the states. This can include Stark mixing in external electric fields [2,4], an induced electric moment by postcollision interaction [5], and the lifetime broadening of nearby atomic levels [3].

In the case of electron- or ion-induced excitation and ionization processes it has long been shown [6] that the orbital angular momentum can be treated as being decoupled from the spin and nuclear angular momenta. Therefore, the coherent excitation of overlapping states with the same angular momentum projections should be considered in these cases. Since the alteration of the angular distribution is an indication of such coherences, systems showing strong alignment in the excitation offer possibilities for their study.

A good candidate where coherence and correlation effects can be studied is the satellite Auger-electron emission following *KL* double ionization of Ne [7–10]. The simultaneous $1s$ and $2p$ ionization of Ne has been studied both by electron [11] and heavy charged particle impact [10,12–14], observing basically no alignment in the former case and strong anisotropy in the latter. The strong anisotropy in the proton impact measurement of [10] allowed us to study the details of the double ionization process of Ne. The underlying reason for the strong alignment is the simultaneous creation of the $1s$ and $2p$ vacancies. Since the $1s$ state is closely localized around the nucleus the simultaneous collisional ionization of the $2p$ state preferentially happens to a specific magnetic state that is strongly localized along the beam direction [15]. Other processes, such as electron shake off after single $1s$ ionization, tend to diminish the net alignment; therefore, the Auger-electron anisotropy can provide details about the relative strength of the contributing processes [10].

The role of coherence and correlation effects in affecting the angular distribution of these transitions has been analyzed by Kabachnik *et al.* [9]. The widths (Γ) of the individual initial double-vacancy states are usually the same magnitudes or larger than their energy splitting (ω). Therefore, the levels belonging to the same multiplet overlap strongly. Mehlhorn and Tauljberg [16] and Bruch and Klar [17] developed the general theory of the angular distribution of electrons from the decay of autoionizing states with an arbitrary ratio between the energy splitting of fine-structure levels and the natural level widths. Kabachnik and coworkers [9] suggested a modification to the general expression for the treatment of the angular distribution that is more convenient for relativistic calculations. Within the multiconfiguration Dirac-Fock (MCDF) approach they have calculated the energies, decay rates, and anisotropy parameters for

*Also at Heliophysical Observatory of the Hungarian Academy of Sciences, P.O. Box 30, H-4010 Debrecen, Hungary. Electronic address: tothla@tigris.klte.hu

†Also at Debrecen University, Experimental Physics Department, Bem tér 18/a, H-4026 Debrecen, Hungary.

‡URL: http://www.atomki.hu

all the *KL-LLL* satellite lines in Ne. It was found that the difference between the calculations based on the nonrelativistic *LS* coupling ($\Gamma \gg \omega$) and the MCDF method ($\Gamma = 0.2$ eV, $\omega \approx 0.1$ eV) was significant. However, the uncertainties of the experimental data [11,14,18] did not allow us to arrive at a definite conclusion at that time.

In the present work a series of high resolution and good statistics for the Ne *KL-LLL* Auger satellite spectra has been used to study the angular distribution properties of these lines. The experimentally determined angular distribution parameters have been accurate enough to analyze the rule of coherence effects. The energies and relative intensities of the satellite Auger lines were determined and compared with theories and with previous experimental data as well.

II. METHOD OF INVESTIGATION

The Auger decay mode is dominant over radiative channels for inner-shell vacancies of low atomic number elements. Therefore, to study the alignment of the $1s2p$ double-vacancy states in Ne we measured the angular distribution of *KL-LLL* satellite Auger electrons after ionization by H^+ and He^+ projectiles. Further argument for taking electron spectra is that a good separation of the neighboring satellite lines can be achieved due to the high energy resolution of electrostatic electron spectrometers.

The angular distribution of the intensity of the outgoing Auger electrons can be expressed as

$$I(\Theta) = I_0\left[1 + \sum_{n=2,even} A_n P_n(\cos\,\Theta)\right], \tag{1}$$

where I_0 is the total Auger-electron intensity ejected into a unit solid angle, Θ is the angle of the ejected Auger electron relative to the beam direction, and P_n is the nth order Legendre polynomial [19]. If one assumes that the ionization and the subsequent decay are independent processes the A_n anisotropy parameters can be written as products [20]

$$A_n = \alpha_n \mathcal{A}_{n0}, \tag{2}$$

where the $\mathcal{A}_{n0}$'s are the alignment parameters of the initial state of the Auger decay and α_n's are the angular anisotropy coefficients. This means that the angular distribution of Auger electrons depends on the alignment of the initial inner-shell vacancy states and on the particular Auger transition that fills them [20].

In our particular case of doubly ionized Ne atoms, the studied $1s^1 2s^2 2p^5$ initial configuration has ^1P and ^3P multiplets. From the selection rules of the Auger process it follows that these initial states can decay into the $1s^2 2s^0 2p^5(^2P)$, $1s^2 2s^1 2p^4(^2S, ^2P, ^2D, ^4P)$, and $1s^2 2s^2 2p^3(^2P, ^2D)$ final states, resulting in 13 different $KL_{2,3}$-$LLL_{2,3}$ Auger satellite lines in the spectra. The most intense lines are those which lead to the $1s^2 2s^2 2p^3(^2P)$ and $1s^2 2s^2 2p^3(^2D)$ final states. Figure 1 shows one of our measured Ne $KL_{2,3}$-$LLL_{2,3}$ Auger spectra, recorded at 165° observation angle with respect to the direction of a 2000 keV He^+ beam. The assignment of the Auger lines are the same as in Refs. [11,18,21], which contain fairly complete identifications of these transitions.

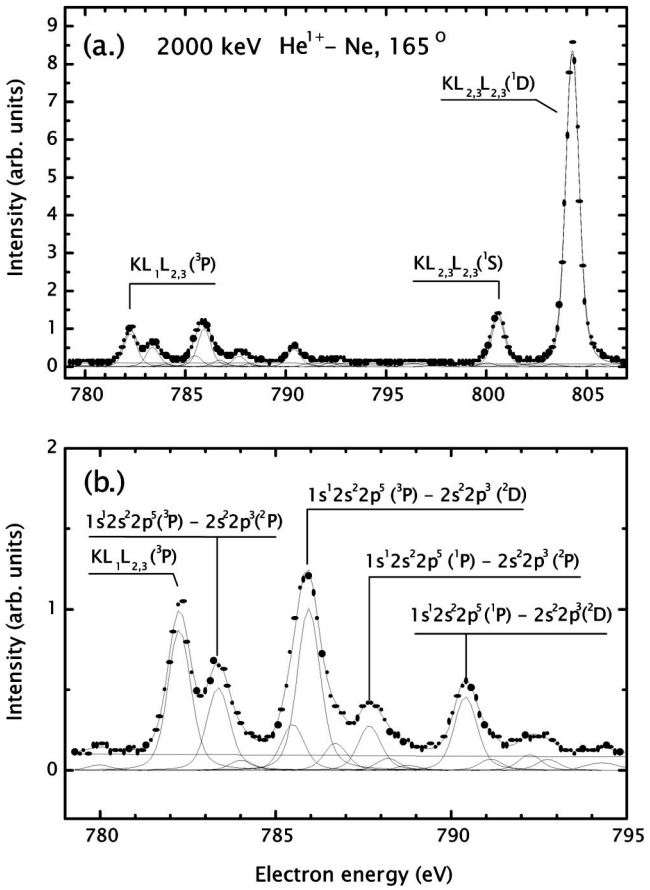

FIG. 1. (a) Part of the Ne $KL_{2,3}$-$LLL_{2,3}$ Auger spectrum. The spectrum was taken at 165° relative to the He^+ beam direction. The projectile energy was 2000 keV. The $KL_{2,3}L_{2,3}(^1D)$, namely the $1s^1 2s^2 2p^6(^2S_{1/2}) \rightarrow 1s^2 2s^2 2p^4(^1D_2)$ diagram line, was used for normalization (see Sec. III). The black circles are the measured values and the solid lines are the fitted curves. (b) Detailed view of the measured satellite lines. For a list of the identified Auger lines see, e.g., Refs. [21,11,18].

In the general case the angular distribution of the Auger electrons can be described with Eq. (1). In the special case of the $^{1,3}P$ initial states only one anisotropy parameter, namely A_{20}, can differ from zero [10]. Therefore, the angular distributions of the observed lines are

$$I(\Theta) = I_0[1 + A_{20} P_2(\cos\,\Theta)]. \tag{3}$$

Based on this simple formula, we fitted the angular distribution of the spectral lines of the $1s^1 2s^2 2p^5(^{1,3}P) \rightarrow 1s^2 2s^2 2p^3(^2P^2D)$ transitions, and determined the angular anisotropy parameters of them. Our aim was to obtain the angular anisotropy coefficients of the individual lines. This could be done by dividing the anisotropy parameters with the alignment parameter of the initial states. Because the ionization is assumed to be spin independent, the A_{20} parameter is the same for all the transitions considered. The experimental determination of the alignment parameter will be described in the following section.

III. EXPERIMENTAL SETUP AND DATA EVALUATION

Our measurements were performed by the ESA-21 triple pass electrostatic electron spectrometer [22]. This facility was made to record the electron spectra at 13 different angles simultaneously relative to the projectile beam direction, in the angular range of $0°-180°$ with 15° increments. The Ne gas jet target was crossed by the beam of the bombarding H^+ and He^+ projectiles, which were produced by the 5-MV Van de Graaf accelerator of ATOMKI. The electrons produced in the collisions passed through the spectrometer and were detected by channel electron multipliers. In our investigations the projectile energy range was 700–2000 keV. The typical vacuum in the target region was about 4×10^{-5} and 5×10^{-7} mbar with and without a gas jet target, respectively. The pressure in the buffer container before the jet inlet was 40 mbar. The gas target was dense enough to obtain good Auger-electron intensity but was rare enough to maintain single-collision conditions. The numerous spectra (142 in total) have been analyzed using the EWA computer code developed by one of the authors [23]. We have shown earlier in [24] that the effect of the postcollision interaction (PCI) is not negligible even at these high projectile energies. In the fitting procedure we applied a five-parameter PCI line shape [25,26] as it was described in detail in Ref. [24]. The Lorentzian widths (0.27 eV, [27]) and the so-called asymmetry parameters for all the lines in a given spectrum were fixed and the widths of the Gaussian spectrometer functions ($\approx$0.55 eV) were proportional to the electron energy. The areas under the PCI shaped curves, that is the intensities of the Auger lines, were obtained from the fits at different observation angles. In the next step the lines were normalized to the isotropic $1s^12s^22p^6(^2S_{1/2})\rightarrow1s^22s^22p^4(^1D_2)$ diagram line. This normalization removed the differences in the detection efficiencies and the geometrical factors at the different observation angles. Figure 2 shows the angular distributions of the examined lines after normalization.

To obtain the A_2 anisotropy parameters, the angular distribution of the normalized intensities was fitted by Eq. (3). To minimize the uncertainty of the fitting, the intensities at 0° were not taken into account. At 0° the interaction of the projectile and the outgoing electron can distort the angular distribution because of the so-called Coulomb-focusing effect [28]. This effect is especially pronounced at the resonant projectile energy (E_p=1473 keV, Fig. 2) where the velocity of the projectile is the same as the velocity of the outgoing Auger electron [24].

As the alignments of the two multiplets ^1P and ^3P are the same for Ne (in *LS* and MCDF calculation [9]), their common $\mathcal{A}_{20}$ parameter can obtained from the anisotropy of a single transition with a known α_2 parameter. In our case we used the $1s^12s^22p^5(^1\mathrm{P})\rightarrow1s^22s^22p^3(^2D)$ line to determine the $\mathcal{A}_{20}$ parameter common to all the observed satellite transitions, because it is the most isolated line in the spectrum, and its α_2 parameter has the exact value of $\sqrt{2}/2$ in both *LS* and *jj* couplings. All other experimental α_2 values were calculated using this $\mathcal{A}_{20}$ parameter and are listed in Table III. The error bars in Table III and throughout the paper include statistical and fitting uncertainties.

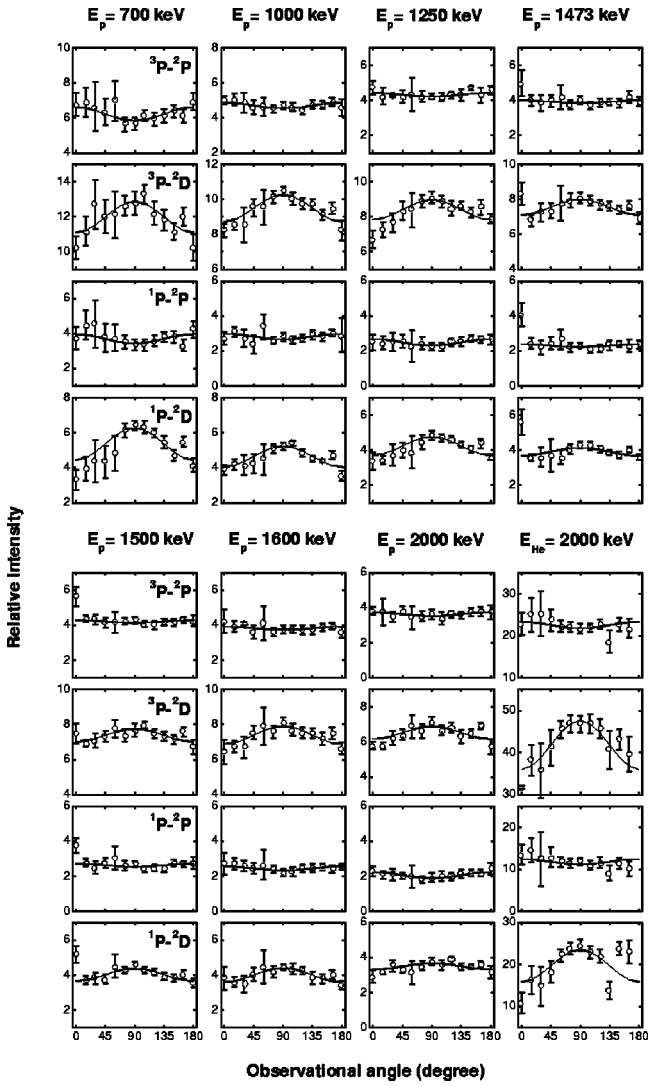

FIG. 2. Angular distributions of the normalized $1s^12s^22p^5(^{1,3}P)\rightarrow1s^22s^22p^3(^2P,^2D)$ line intensites in the case of H^+ and He^+ bombardment. The solid lines are the fitted curves by Eq. (3).

IV. RESULTS AND DISCUSSION

A. Energies and intensities of the satellite transitions

The energies and intensities of the Ne *KL-LLL* Auger satellite lines have already been measured in several collision systems with different charged particle projectiles [11,18,21,29–31]. In Table I our measured line energies are compared to the results of other high-resolution experiments performed with electron [11] and ion beams [18] together with the recent MCDF calculation results [9]. Our results were determined as the weighed means of the measured energies of the investigated lines in 142 different spectra. There is a general agreement between the measured line energies but not within the published error bars. This might be related to the different energy calibration procedures. In experiment [18] and also in the case of the MCDF calculation [9] the energy of the $KL_{2,3}L_{2,3}{}^1D$ diagram line was fixed to 804.50 eV. We also followed this procedure in our evalua-

TABLE I. Measured and calculated energies for $1s^1 2s^2 2p^5(^{1,3}P) \rightarrow 1s^2 2s^2 2p^3(^2P, ^2D)$ satellite Auger transitions. For details see text.

	Energy (eV)			
	Theory	Experiment		
Transition	[9]	[18]	[11]	This work
$^3P \rightarrow {}^2P$	786.18	783.29(1)	783.45(8)	783.36(3)
$^3P \rightarrow {}^2D$	788.35	785.86(2)	786.04(8)	785.97(3)
$^1P \rightarrow {}^2P$	790.59	787.84(2)	787.83(8)	787.69(3)
$^1P \rightarrow {}^2D$	792.56	790.46(1)	790.51(8)	790.48(2)

TABLE II. Measured and calculated relative intensities for $1s^1 2s^2 2p^5(^{1,3}P) \rightarrow 1s^2 2s^2 2p^3(^2P, ^2D)$ satellite Auger transitions normalized to the sum of the two transitions from the same initial state.

	Relative intensity (%)				
	Theory		Experiment		
Transition	[32]	[9]	[18]	[11]	This work
$^3P \rightarrow {}^2P$	34.8	33.1	27.6(6)	34.6(13)	34.6(4)
$^3P \rightarrow {}^2D$	65.2	66.9	72.4(6)	65.4(13)	65.4(4)
$^1P \rightarrow {}^2P$	34.9	33.2	35.1(10)	36.1(17)	37.8(7)
$^1P \rightarrow {}^2D$	65.1	66.8	64.9(10)	63.9(17)	62.2(7)

tion. However, in [11] a value of 804.30 eV was used for the same Auger-electron energy. This 0.2 eV uncertainty in the position of the $KL_{2,3}L_{2,3}{}^1D$ line is almost an order of magnitude larger than the error bars from counting statistics and fitting uncertainties. There is a rather big (2–3 eV) difference on the absolute energy scale between the MCDF calculation [9] and the experiments. The agreement is significantly better for the line separations.

Experimental and theoretical data for the relative yields of the same satellite lines are presented in Table II. There is a good agreement between experiments and theories. We note that, contrary to earlier expectations [32], the relative intensities of the Auger satellite lines seem to be not sensitive to configuration interactions in the final ionic states. There is no significant difference between the LS and MCDF [9,32] calculations for the relative yields.

B. Angular anisotropy coefficients

According to theoretical expectations [9], the anisotropy of an Auger transition is sensitive to the fine details of the decay process. Measuring the angular distribution of Auger emission provides valuable information for the above details. The anisotropy is considerably sensitive to the overlap of different electronic states and to the coupling of the spin and the orbital angular momenta in the initial and final states of the Auger transition. Coherent excitation of overlapping atomic states can lead to interference effects [1] generally reducing the anisotropy of the subsequent Auger decay [33]. The first theoretical descriptions of the anisotropy of Ne *KL-LLL* satellite Auger transition were based purely on *LS* coupling ($\Gamma \gg \omega$), single-configuration Hartree-Fock calculations. These theories cannot describe the anisotropy of the Auger emission quantitatively [11,14,34]. More sophisticated descriptions account for spin-orbit interactions, and the fact that the widths of the individual initial double-vacancy states are often comparable or larger than their energy splitting ($\Gamma \geqslant \omega$) [35–40]. Later, Kabachnik and his co-workers [9] applied the relativistic MCDF method to treat the anisotropy of Auger emission from overlapping states. Experimentally so far only one measurement [14] has been devoted to study the problem. Since the difference between the nonrelativistic *LS* coupling and Kabachnik's MCDF calculations is smaller than the uncertainties of the experiment [14], in the present work, we performed more accurate measurements with higher resolution.

The experimental angular anisotropy coefficients (α_2) have been determined from a large set of high-resolution spectra taken at different projectile energies and observational angles (Table III). It can be seen from Table III and Fig. 3 that the (α_2) coefficients measured with different projectiles at different impact energies have about the same values. The only exception is the case of 2000 keV proton impact, where the small anisotropy values (see Fig. 2) cannot provide reliable α_2 data at the present level of experimental accuracy. This observed impact energy independence indicates that our assumption for the separability of the excitation and the Auger decay processes is valid. The only sign of the nonseparability of the excitation and the decay processes is the already mentioned small Coulomb focusing effect at 0° Fig. 2. Accordingly we averaged the (α_2) coefficients due to different projectiles and impact energies for each individual transition. The averaged data compared with other experimental results [14] and different theoretical calculations [9,14] are presented in Table IV and Fig. 3.

There are three different sets of theoretical calculations presented in Fig. 3. The first set is a single configuration

TABLE III. Experimental angular anisotropy coefficients (α_2) for the studied transitions in the case H^+ and He^+ (signed by †) impact.

	Angular anisotropy coefficients (α_2)							
	Projectile energy (keV/amu)							
Transition	500†	700	1000	1250	1473	1500	1600	2000
$^3P \rightarrow {}^2P$	−0.14(7)	−0.28(20)	−0.20(27)	−0.16(27)	−0.23(67)	−0.15(37)	−0.18(38)	−0.45(108)
$^3P \rightarrow {}^2D$	0.51(7)	0.32(16)	0.46(22)	0.40(25)	0.70(68)	0.40(34)	0.49(36)	0.82(111)
$^1P \rightarrow {}^2P$	−0.21(13)	−0.33(32)	−0.32(44)	−0.45(53)	−0.42(107)	−0.27(60)	−0.38(59)	−1.28(209)

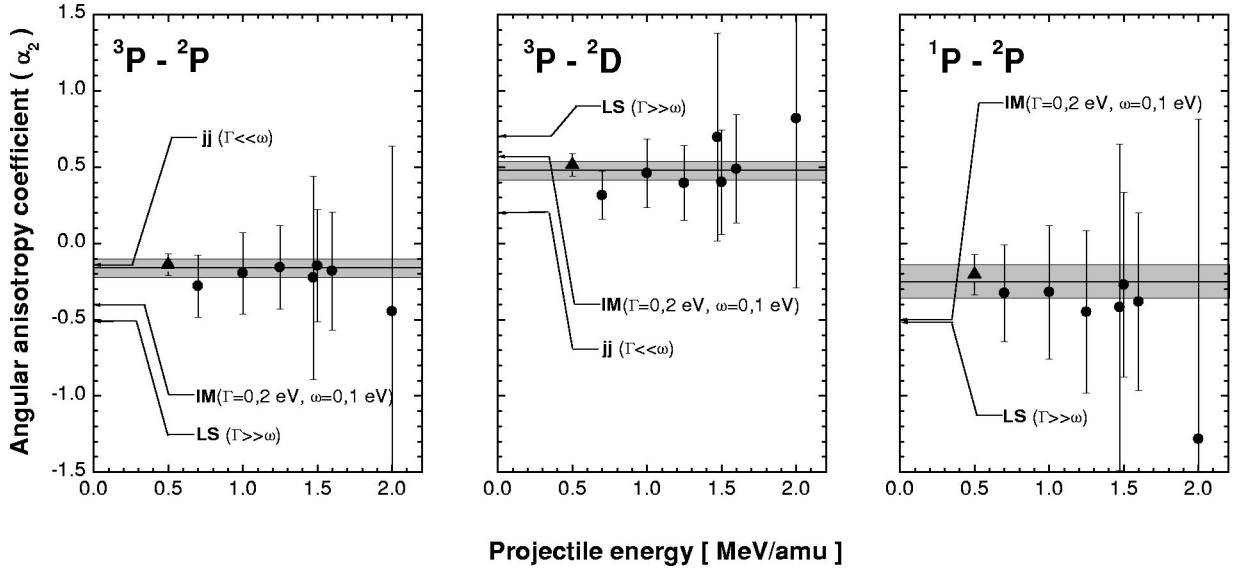

FIG. 3. Experimental angular anistropy coefficients (α_2) for the $1s^12s^22p^5(^{1,3}P)\rightarrow 1s^22s^22p^3(^2P,^2D)$ satellite Auger transitions in the case of He^+ (signed by solid triangle) and H^+ (signed by solid circle) projectile, as a function of the impact energy. Solid line with gray area is the weighed mean of the experimental α_2 coefficients and its sample standard deviation. The theoretical α_2 coefficients within the framework of pure LS coupling ($\Gamma \gg \omega$) calculations [14] and MCDF method [IM coupling ($\Gamma = 0.2$ eV, $\omega \approx 0.1$ eV)] and *jj* coupling ($\Gamma \ll \omega$) [9] are indicated in the figure.

nonrelativistic calculation in the *LS* coupling scheme ($\Gamma \gg \omega$) [14]. The second set of theoretical results has been calculated with coherently excited and partially overlapping ($\Gamma = 0.2$ eV, $\omega \approx 0.1$ eV) initial states using the MCDF method [9]. The third set is also a MCDF calculation performed in a pure *jj* coupling scheme ($\Gamma \ll \omega$) [9]. In the following, the above three calculations will be denoted by the abbreviations "*LS*," "IM" (intermediate) and "*jj*," respectively. In the case of the $1s^12s^22p^5(^1P)\rightarrow 1s^22s^22p^3(^2P)$ transition the difference between the LS ($\Gamma \gg \omega$) and the IM ($\Gamma = 0.2$ eV, $\omega \approx 0.1$ eV) calculations is less than the uncertainty of our present experimental result (Table IV and Fig. 3) (similarly to [14]). However, in the case of the $1s^12s^22p^5(^3P)\rightarrow 1s^22s^22p^3(^2D)$ transition, our experimental angular anisotropy coefficient (α_2) positively favors the IM ($\Gamma = 0.2$ eV, $\omega \approx 0.1$ eV) results [9] (Table IV and Fig. 3). For the case of the $1s^12s^22p^5(^3P)\rightarrow 1s^22s^22p^3(^2P)$ transition the measured anisotropy parameter also favors the IM results ($\Gamma = 0.2$ eV, $\omega \approx 0.1$ eV) against those of the *LS* coupling calculations. However, in this case better agreement was found with the pure *jj* coupling calculations ($\Gamma \ll \omega$) [9] (Table IV and Fig. 3).

The present experiments agree better with the results of the MCDF calculations performed in the intermediate and *jj* coupling schemes than those of the single configuration *LS* coupling calculations. This fact supports the conclusion that the spin orbit and the configuration interactions are not negligible for the studied transitions.

V. SUMMARY

We measured the energies, intensities, and the angular distributions of the ^3P-^2P, ^3P-^2D, and ^1P-^2P satellite Auger electrons from the Ne target. 500–2000 keV/amu He^+ and H^+ ions were used as projectiles, and comparison was made with another experiment [14] and with theories [9,14].

From the angular distributions of the studied transitions we have determined the angular anisotropy coefficients (α_2) and shown that the accurate experimental investigation of the α_2 is a suitable method for testing the different levels of theoretical description for the Auger decay.

TABLE IV. Experimental and theoretical angular anisotropy coefficients (α_2), averaged over the 500–2000 keV/amu projectile energy range.

	Theory			Experiment	
		MCDF calculation [9]			
	LS coupling [14]		*jj* coupling		
Transition	($\Gamma \gg \omega$)	($\Gamma = 0.2$ eV, $\omega \approx 0.1$ eV)	($\Gamma \ll \omega$)	[14]	This work
$^3P \rightarrow {}^2P$	−0.511	−0.405	−0.139	−0.75(20)	−0.16(6)
$^3P \rightarrow {}^2D$	0.707	0.573	0.196	0.62(15)	0.48(6)
$^1P \rightarrow {}^2P$	−0.511	−0.498	⋯	−0.44(23)	−0.25(11)

We found that pure *LS* coupling calculations could not reproduce the experimental anisotropy coefficients of Ne. The present experimental results are in better agreement with those calculations where the overlap between the fine structure component of the $^3P_{0,1,2}$ double ionized state of Ne is supposed to be comparable ($\Gamma = 0.2$ eV, $\omega \approx 0.1$ eV [9]) to or larger ($\Gamma \ll \omega$) than their natural widths. The results suggest that mostly partially overlapping states need to be taken into account.

ACKNOWLEDGMENT

This work was supported by the Hungarian National Science Foundation (Grant Nos. OTKA: T03294, T037203).

[1] U. Fano and J. H. Macek, Rev. Mod. Phys. **45**, 533 (1973).
[2] H. J. Andrä, Phys. Rev. Lett. **25**, 325 (1970).
[3] K. Ueda, Y. Shimizu, N. M. Kabachnik, I. P. Sazhina, R. Wehlitz, U. Becker, M. Kitajima, and H. Tanaka, J. Phys. B **32**, 291 (1999).
[4] J. Macek, Phys. Rev. Lett. **23**, 1 (1969).
[5] J. Burgdörfer, Phys. Rev. A **24**, 1756 (1981).
[6] I. C. Percival and M. J. Seaton, Philos. Trans. R. Soc. London, Ser. A **251**, 113 (1958).
[7] N. M. Kabachnik, in *Proceedings of the XVIIIth International Conference on the Physics of Electronic and Atomic Collisions, Aarhus*, edited by T. Andersen, B. Fastrup, F. Folkmann, H. Knudsen, and N. Andersen (AIP, New York, 1993), Vol. 295, p. 73.
[8] V. Schmidt, in *Proceedings of the XVIth International Conference on X-ray and Inner-Shell Process, Debrecen*, edited by L. Sarkadi and D. Berényi (Atomki, Debrecen, 1993), Vol. 87, p. 241.
[9] N. M. Kabachnik, J. Tulkki, H. Aksela, and S. Ricz, Phys. Rev. A **49**, 4653 (1994).
[10] E. Takács, S. Ricz, J. Végh, I. Kádár, J. Pálinkás, B. Sulik, L. Tóth, D. Berényi, and N. M. Kabachnik, Phys. Rev. A **50**, 1197 (1994).
[11] A. Albiez, M. Thoma, W. Weber, and W. Mehlhorn, Z. Phys. D: At., Mol. Clusters **16**, 97 (1990).
[12] S. Ricz, I. Kádár, V. A. Shchegolev, D. A. Varga, J. Végh, D. Berényi, G. Hock, and B. Sulik, J. Phys. B **19**, 411 (1986).
[13] I. Kádár, S. Ricz, B. Sulik, D. Varga, J. Végh, and D. Berényi, Nucl. Instrum. Methods Phys. Res. A **40/41**, 60 (1989).
[14] S. Ricz, J. Végh, I. Kádár, B. Sulik, D. Varga, and D. Berényi, Nucl. Instrum. Methods Phys. Res. B **61**, 411 (1991).
[15] K. A. Jamison and P. Richard, Phys. Rev. Lett. **38**, 484 (1977).
[16] W. Mehlhorn and K. Taulbjerg, J. Phys. B **13**, 445 (1980).
[17] R. Bruch and H. Klar, J. Phys. B **13**, 1363 (1980).
[18] I. Kádár, S. Ricz, J. Végh, B. Sulik, D. Varga, and D. Berényi, Phys. Rev. A **41**, 3518 (1990).
[19] B. Cleff and W. Mehlhorn, J. Phys. B **7**, 593 (1974).
[20] E. G. Berezhko and N. M. Kabachnik, J. Phys. B **21**, 963 (1988).
[21] M. O. Krause, T. A. Carlson, and W. E. Moddeman, J. Phys. (Paris) **32**, 139 (1971).
[22] D. Varga, I. Kádár, S. Ricz, J. Végh, A. Kvér, B. Sulik, and D. Berényi, Nucl. Instrum. Methods Phys. Res. A **313**, 163 (1992).
[23] J. Végh, in *Proceedings of the 6th European Conference on Applications of Surface and Interface Analysis, Montreaux*, edited by H. J. Mathieu, B. Reidl, and D. B. Chichester (Wiley, Chichester, 1996), p. 679.
[24] E. Takács, L. Sarkadi, S. Ricz, B. Sulik, and L. Tóth, J. Phys. B **24**, 381 (1991).
[25] M. Y. Kuchiev and S. A. Scheinerman, Zh. Eksp. Teor. Fiz. **90**, 1680 (1986).
[26] P. van der Straten and R. Morgenstern, J. Phys. B **19**, 1361 (1986).
[27] M. O. Krause and J. H. Oliver, J. Phys. Chem. **8**, 329 (1979).
[28] G. Víkor, S. Ricz, B. Sulik, L. Tóth, A. Kövér, and J. Végh, J. Phys. B **29**, 787 (1996).
[29] W. M. H. Korber, Z. Phys. **191**, 217 (1966).
[30] D. L. Methews, B. M. Johnson, J. J. Mackey, L. E. Smith, W. Hodge, and C. F. Moore, Phys. Rev. A **10**, 1177 (1974).
[31] M. Levasalmi, H. Aksela, and S. Aksela, Phys. Scr. **41**, 119 (1992).
[32] V. Schmidt, in *Proceedings of the XVIth International Conference on Inner-Shell Ionization Phenomena and Future Applications, Atlanta*, edited by R. Fink, S. Manson, J. Palms, and P. V. Rao (U.S. Atomic Energy Commission, Oak Ridge, TN, 1973), Vol. 1, p. 548.
[33] W. Mehlhorn (unpublished).
[34] N. M. Kabachnik, J. Phys. B **21**, 267 (1988).
[35] N. M. Kabachnik, B. Lohmann, and W. Mehlhorn, J. Phys. B **24**, 2249 (1991).
[36] M. H. Chen, Phys. Rev. A **45**, 1684 (1992).
[37] J. Tulkki, N. M. Kabachnik, and H. Aksela, Phys. Rev. A **48**, 1277 (1993).
[38] U. Hergenhahn, B. Lohmann, N. M. Kabachnik, and U. Becker, J. Phys. B **26**, 117 (1993).
[39] M. H. Chen, Phys. Rev. A **47**, 3733 (1993).
[40] J. Tulkki, H. Aksela, and N. M. Kabachnik, Phys. Rev. A **48**, 2957 (1993).